Consistent Anomaly Detection and Localization of Multivariate Time Series via Cross-Correlation Graph based Encoder-Decoder GAN

Article *in* IEEE Transactions on Instrumentation and Measurement · December 2021

DOI: 10.1109/TIM.2021.3139696

5 authors, including:

Liang Haoran
Chinese Academy of Sciences
11 PUBLICATIONS **25** CITATIONS

SEE PROFILE

Lei Song
Chinese Academy of Sciences
26 PUBLICATIONS **81** CITATIONS

SEE PROFILE

Consistent Anomaly Detection and Localization of Multivariate Time Series via Cross Correlation Graph-Based Encoder–Decoder GAN

Haoran Liang, Lei Song, Junrong Du, Xuzhi Li, and Lili Guo

***Abstract*— Multivariate time series is widely derived from industrial facilities, such as power plants, manufacturing machines, spacecraft, digital devices, and so on, and anomaly detection and location is of great importance to industrial preventive maintenance. However, anomalies in multivariate time series always result from their unusual change of temporal or correlative features, and it is challenging to capture these complex characteristics. Besides, achieving consistent anomaly detection and location performance is also a tricky issue. In this article, a novel anomaly detection and location framework that combines generative adversarial networks and autoencoder is proposed to capture time dependent and correlation features of multivariate time series with the need of anomalous sequences. First, multitime scale correlation computation is utilized to encode multivariate time series into multiple cross correlation graphs, which can be fed into the proposed deep architecture for extracting more distinguishable features. On this basis, a robust cost function with multiple loss issues is designed, and reconstruction matrix deviation from original space of encoder–encoder structure is utilized to detect and locate abnormal time series, ensuring the consistency of detection and location tasks and the framework reliability. Extensive experiments on five industrial datasets are conducted to indicate our model is a generic and excellent framework for anomaly detection and location of multivariate time series.**

***Index Terms*— Anomaly detection and location, cross correlation graph, encoder–decoder GAN, multivariate time series.**

I. Introduction

ADVANCED techniques have provided industrial systems with more efficient and reliable monitoring devices, and various sensors are equipped to collect multivariate time series with different attributes, scales, and characteristic [1]. Anomaly detection of multivariate time series is an applicable way to discover the failures and monitor the health of industrial facilities [2]–[5]. However, multivariate time series always refer to contextual or collective anomalies, and it is challenging for anomaly detection models to catch the unusual changes of temporal and correlative features among multivariate time series. Besides, anomalous data in industrial fields are always unavailable, which makes supervised models are infeasible [6]. In contrast, as industrial systems demand higher reliability and stability, maintainers urgently need to locate detailed sensors, further providing more specific operational advices to device maintainers [7].

In recent years, amount of semi-supervised or unsupervised anomaly detection algorithms [8], such as clustering/density-based algorithms, ensemble algorithms, and probabilistic algorithms have been developed, but two respects should be concerned. First, most classical algorithms, such as k-nearest neighbor (KNN) [9], Gaussian mixture model (GMM) [10], and one-class SVM [11], are only good at dealing with 1-D time series and are not skilled at capturing the temporal and correlative features among multivariate time series. Second, most existing algorithms focus on anomaly detection but ignore to locate anomalous dimensions. Actually, some anomaly location models like Opprentice [12], EDAGS [13], DONUT [14], and ROCKA [15] always need to build individual models for each time series, which can result in large overhead of model selection, parameter tuning, and model training in practice.

Fortunately, deep learning (DL) has become a state of the art in time series modeling owe to its strong nonlinear expression ability and flexibility in data modeling [16]. Long short-term memory (LSTM)-based VAE-GAN [17] takes the advantages of the mapping ability of the encoder and the discrimination ability of the discriminator simultaneously, and LSTM networks are used as the encoder, the generator, and discriminator for detect anomalies via reconstruction difference and discrimination results. According to the imbalanced time series, a novel GAN-based anomaly detection approach with an encoder–decoder–encoder three-subnetwork generator is developed, and the anomaly score computed through the apparent and latent loss is designed for anomaly detection [18]. Efficient GAN-based anomaly detection (EGBAD) leverages GAN that simultaneously learn an encoder during training, and efficient detection results are achieved on image and network intrusion datasets [19]. Multivariate anomaly detection with

AQ:1 Manuscript received August 19, 2021; revised November 22, 2021; accepted December 19, 2021. The Associate Editor coordinating the review process was Qiang Miao. *(Haoran Liang and Lei Song contributed equally to this work.) (Corresponding author: Lei Song.)*

AQ:2 Haoran Liang and Junrong Du are with the Key Laboratory of Space Utilization, Technology and Engineering Center for Space Utilization, Chinese Academy of Sciences, Beijing 100094, China, and also with the University of Chinese Academy of Sciences, Beijing l00049, China.

Lei Song and Xuzhi Li are with the Key Laboratory of Space Utilization, Technology and Engineering Center for Space Utilization, Chinese Academy of Sciences, Beijing 100094, China (e-mail: songlei@csu.ac.cn).

Lili Guo is with the Key Laboratory of Space Utilization, Technology and Engineering Center for Space Utilization, Chinese Academy of Sciences, Beijing 100094, China, and also with the School of Software, Tsinghua University, Beijing 100084, China.

Digital Object Identifier 10.1109/TIM.2021.3139696

GAN (MAD-GAN), using LSTM recurrent neural networks (LSTM-RNN) structure, is proposed to capture temporal features of multivariate time series distributions, and a novel anomaly score called DR-score is designed to detect anomalies via discrimination and reconstruction [20]. Actually, studies above focus on developing accurate and effective anomaly detection models and ignore to locate the detailed anomalous sensors from multivariate time series, failing to provide specific operational devices for industrial maintainers [21].

Among all anomaly detection algorithms, some models capable of locating abnormal parameters have been applied in many fields. DONUT [14] builds individual encoder–decoder structure for each dimensional time series in web applications, which detect and locate anomalies among multiple time series. Actually, when the dimension of time series is large, DONUT needs to build number of submodels and costs large overhead. Afterward, ROCKA [15] is designed to train a DONUT through clustering results. Although ROCKA succeeds to reduce the computing overhead, its essence is still to build many submodels for each time series. AnoGAN is the first GAN-based anomaly detection framework for lesion detection of unknown medical images [22], and then AnoGAN is improved as an efficient anomaly approach f-AnoGAN, of which the training consists of GAN training and encoder training based on the trained GAN. The weighted reconstruction error of original and latent space is defined as anomaly detection indicator, and the former is adopted as location indicator [23]. Therefore, the inconsistent index may lead to performance differences of anomaly detection and location. Likewise, GANomaly is proposed to combine encoder–decoder–encoder and GAN structures, and anomaly detection and location, respectively, adopt reconstruction errors in the latent and original space, resulting in the same problem above [24]. Besides, multiscale convolutional recurrent encoder–decoder (MSCRED) with structure ConvLSTM is developed to perform anomaly detection and location for multivariate time series [7]. However, its drawbacks mainly manifest in the following respects, such as poor robustness of feature extraction under noise disturbance, gradient vanishing during training process, and low computing efficiency.

In this article, a novel framework cross correlation graph-based encoder–decoder GAN (CCG-EDGAN) is proposed to provide a consistent framework for unsupervised anomaly detection and location of industrial multivariate time series. To the best of our knowledge, it is the first time that detects and locates multivariate time series using encoder–decoder GAN model. The main contributions of our work are described below.

First, a novel framework CCG-EDGAN is proposed for unsupervised anomaly detection and location of multivariate time series. Multitime scale sliding window-based cross correlation computation is adopted to transform multivariate time series into multiple cross correlation graphs, which are fed into encoder–decoder GAN architecture to learn the inner correlative features of multivariate time series. Furthermore, residual connection is designed to avoid deep structure degradation for better convergence performance, and noise module is introduced into encoder–decoder GAN framework, increasing the encoding randomness and slowing down the mode collapse of GAN architecture.

Second, multiple loss issues are designed to create a cost function, and the function can restrain the optimization direction of CCG-EDGAN from the latent space and the original space simultaneously, contributing to achieve better model parameters. Meanwhile, residual feature matrix from original space is developed as a generic indicator to detect and locate anomalous dimensions from multivariate time series, achieving consistent and excellent results on detection and location tasks.

Finally, experiments on five industrial datasets are implemented to verify the effectiveness of the proposed framework in anomaly detection and location of multivariate time series, and the results indicate that our framework is superior to comparison models in terms of detection and location performance. Furthermore, ablation study is conducted to demonstrate the effective function of residual connection and noise module.

This article is structured as follows. Section II analyzes related work and the overview of the proposed framework. Section III describes the detailed structures of the proposed framework. The experiments and discussions are detailed in Section IV. Finally, the conclusion is listed in Section V.

II. Methodology

A novel framework CCG-EDGAN is proposed in this article, which consists of three following parts (Fig. 1): (a) preprocessing module, (b) generator, and (c) discriminator. The preprocessing aims to transform multivariate time series into multitime scale cross correlation graphs, which are fed into encoder–decoder GAN architecture to learn sequential correlation features among multiple time series efficiently. The Generator is responsible for generating the most similar fake time series via the encoding and reconstruction of encoder–decoder–encoder structure, which is conducive to better capture the inner features of sequential cross correlation graphs. Moreover, noise module is added into the input of generator to improve the diversity of reconstructed samples. Discriminator refers to a classical classification architecture, attempting to distinguish whether the input is a real or reconstructed data. Besides, residual connection modules are designed to improve the representation ability and convergence performance of deep model. Finally, the reconstruction matrix deviation from input original space through encoder–decoder structure is utilized as the consistent indicator for anomaly detection and location tasks. Fig. 1 shows the graphical illustration of CCG-EDGAN.

III. Model Development

A. Multivariate Time Series Processing

Many previous studies show that the correlation characteristic of different pairs among multivariate time series is a critical attribute to represent the system status [25], [26], and any type of anomaly, such as point, contextual, and collective anomaly can be shown as a change in intercorrelations of multivariate time series. Therefore, cross correlation computation which has been verified as an effective preprocessing method in our previous work [27] is used in this work. In the preprocessing

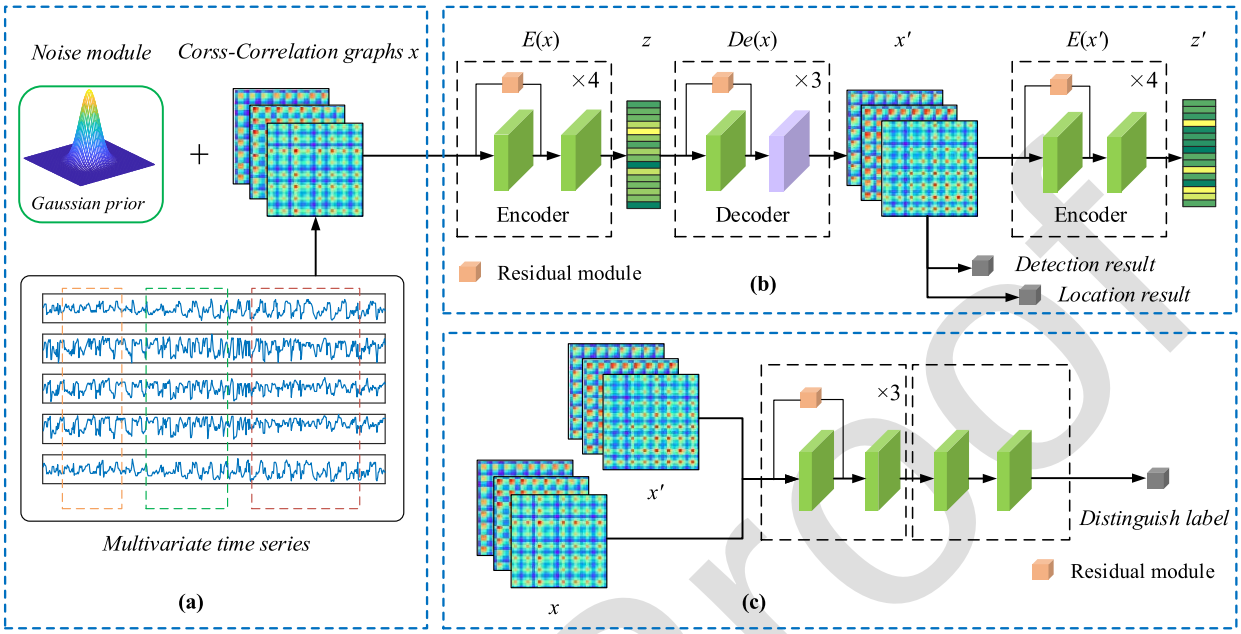

Fig. 1. Graphical illustration of the CCG-EDGAN for industrial multivariate time series anomaly detection and location.

module, signature matric S^t is utilized to encode multivariate time series at each time t via sliding window-based sequence segment from $t-w$ to t [28], and w represents the length of the sliding window. Signature series at current time t is X_t, and therein its two sequences are $X_i^t = (x_i^{t-w}, x_i^{t-w+1}, \ldots, x_i^t)$ and $X_j^t = (x_j^{t-w}, x_j^{t-w+1}, \ldots, x_j^t)$, which are derived from a w length sliding window segment. As described above, signature matrices S^t and its details (1) are given below

$$S^t = \begin{Bmatrix} s_{11}^t & s_{12}^t & \cdots & s_{1w}^t \\ s_{21}^t & s_{22}^t & \cdots & s_{2w}^t \\ \vdots & \vdots & \vdots & \vdots \\ s_{n1}^t & s_{n2}^t & \cdots & s_{nw}^t \end{Bmatrix}, \quad s_{ij}^t = \frac{\sum_{\delta=0}^{w} x_i^{t-\delta} x_j^{t-\delta}}{k} \tag{1}$$

where w represents the length of the sliding window, and k is an experiential coefficient related to w, which means S_{ij}^t can be considered as the mean of dot product for two sequential time series. To characterize the latent features of multivariate time series under multitime scale, three cross correlation graphs are conducted with different length sliding windows ($w = 10$, 30, 60) at each time step. As a result, any unusual changes of cross correlation graph may represent the anomalous inner correlation features of abnormal sequences among multivariate time series.

B. Architecture Design

CCG-EDGAN consists of generator and discriminator, and therein the generator contains a noise module, two encoders (E and E'), and a decoder (De). The encoder (E) and decoder (De) are combined as encoder–decoder structure, and thus Generator aims to learn the input cross correlation graph and reconstruct it via encoder and decoder network. First, Generator reads a cross correlation graph $x \in R^{w \times h \times c}$, and forward passes x to first encoder E. Under the action of convolutional layers followed by batch normalization, LeakyReLU activation, and residual connection, E downscales x by mapping it to a vector $z \in R^d$, which is the representation of x in the latent space. The decoder De utilizes convolutional transpose layers, ReLU activation, batch normalization, and residual connection with a Tanh layer at the end to reconstruct input x as x' from z. The second encoder network E' is similar in function to E except that E' maps x'–z. Different from vanilla GANs, input of CCG-EDGAN is the sample rather than the noise sampled from predistribution, and the randomness of CCG-EDGAN will be reduced, which may result in model collapse of GAN framework. To overcome the problems above, the noise module is developed in Generator to merge noise sampled from normal distribution into input samples.

In general, cross correlation graph is fed into CNN structure, of which convolution kernel performs a convolution operation and outputs a feature map. Then, the feature map is processed through downsampling, and the output of downsampling will be nonlinear mapped via activation function. Actually, multiple convolution layers are stacked to extract the features of multivariate time series at different levels, and different activation functions are adopted in different modules. As in our framework, the encoder uses LeakyReLU, and the last layer of and the other layers of decoder, respectively, adopt Tanh and ReLU. As a result, the inner correlative attribute of multivariate time series is gradually learned step by step.

Meanwhile, discriminator is considered as a classical classifier with convolutional layers to conduct batch normalization. And then LeakyReLU activation and residual connection of discriminator are developed and the final layer network uses the Sigmoid activation function to map the input to [0, 1], which represents the possibility that the input is judged as fake sample.

C. Adversarial Training

Actually, anomalous samples cannot be well reconstructed after the forward propagation in generator of CCG-EDGAN, while the framework is only trained through normal samples

and its parametrization is not suitable for generating abnormal samples. In this case, the samples with high reconstruction errors will be recognized as anomalies. To validate such hypothesis, we design the cost function by combining multiple loss items, each of which optimizes individual subnetworks.

1) Discriminator Loss: We choose the discriminator loss function of vanilla GANs in this article. Specifically, the closer the reconstructed sample is to the input sample, the output of the discriminator is closer to 1. On the contrary, the greater the difference between the reconstructed sample and the input sample, the output of the discriminator is closer to 0. As a result, $L_{\text{discriminator}}$ is defined as follows:

$$L_{\text{discriminator}} = \log D(x) + \log(1 - D(x')). \tag{2}$$

2) Feature Matching Loss: We follow anomaly detection algorithms in [28] and [29] and adopt feature matching strategy to design feature matching loss, which refers to the use of the intermediate feature representation of discriminator to replace the output of the last layer to construct loss function. Feature matching loss is constructed via calculating L_1 distance of the cross correlation graphs output from the penultimate layer of discriminator, shown as follows:

$$L_{\text{fm}} = E_{x-p_x} \left\| D_{\text{feat}}(x) - D_{\text{feat}}(x') \right\|_1. \tag{3}$$

3) Encoding Loss: The encoding loss is used to represent the difference between the latent space variables z and z'. Referring to the article [30], the Pearson correlation is calculated as encoding loss to describe the difference between z and z', and thus the encoding loss is defined as follows:

$$L_{\text{enc}} = \frac{\sum_{i=1}^{n_z} (z_i - \text{avg}(z))\left(z_i' - \text{avg}(z')\right)/n_z}{\text{std}(z) \times \text{std}(z')}. \tag{4}$$

4) Reconstruction Loss: Except for the three loss functions of $L_{\text{discriminator}}$, L_{fm}, and L_{enc}, the generator is also optimized toward learning original information about input signature matrix. Therefore, the reconstruction loss L_{rec} is constructed in original data space and it is designed to penalize the Generator via the L_1 distance between the input cross correlation graph x and the reconstruction graph x'. L_{rec} is defined as follows:

$$L_{\text{rec}} = E_{x \sim p_x} \left\| x - x' \right\|_1. \tag{5}$$

As stated, we integrate L_{fm}, L_{enc}, and L_{rec} to construct the total loss of generator, shown in (6) and therein w_1–w_3 are the weighting parameters adjusting the impact of individual losses to $L_{\text{generator}}$

$$L_{\text{Generator}} = w_1 \times L_{fm} + w_2 \times L_{\text{rec}} + w_3 \times L_{\text{enc}} \tag{6}$$

D. Anomaly Detection and Location

In the testing stage, CCG-EDGAN utilizes L_{rec} to score a given input in both anomaly detection and location tasks to achieve consistent performance. Therefore, according to a testing data $\widehat{x}$, the detection score $A(\widehat{x})$ and location score $D(\widehat{x})$ are defined as (7) and (8). Once the given detection score $A(\widehat{x})$ exceeds the predefined threshold, the data $\widehat{x}$ will be judged as an abnormal sample. Similarly, the location score $D(\widehat{x})$ is an array that records abnormal dimensions which can help to locate anomalous sensors. The specific process of anomaly detection and location is shown in Table I

TABLE I
PSEUDOCODE OF ANOMALY DETECTION AND LOCATION

Algorithm 1: Anomaly detection and location of MCCG-AED

Input:
Testing sample x, reconstruction sample x' ;
Output:
Anomaly detection result label and anomaly diagnosis result array;
Function Anomaly Location (S)
  $S \leftarrow abs(x - x')$
  if $S > threshold_A$ **then**
    label←1
  else
    label←0
  end if
  row←length (S)
  for i = 0→row-1 **do**
    $D[i]$←sum($S[i,:]$)
  end for
  $threshold_D$←percentage (D,90)
  for i= 0→row-1 do
  if D[i]>$threshold_D$ then
    array.append (i)
  end if
 end for
 return label, array
end function

$$A(\widehat{x}) = \sum_{i}^{w} \sum_{j}^{h} \left\| \widehat{x_{ij}} - \text{De}(E(\widehat{x_{ij}})) \right\|_1 \tag{7}$$

$$D(\widehat{x}) = \sum_{i}^{w} \left\| \widehat{x_{ij}} - \text{De}(E(\widehat{x_{ij}})) \right\|_1. \tag{8}$$

IV. EXPERIMENTS AND DISCUSSION

A. Datasets Description

Three public datasets satellite dataset, steam turbine dataset, power consumption dataset, and two real datasets gamma polarization detector dataset and wind turbine dataset are used in this article. All datasets includes labels, and the detailed information of datasets are shown in Table II.

1) *Satellite dataset*[1]*:* The satellite dataset is a benchmarking unsupervised anomaly detection dataset provided by Harvard University. This dataset has been obtained from multiple sources and are mainly based on datasets originally used for supervised machine learning. This dataset includes multiple telemetry data collected from some satellite, containing 36 attributes with normal and abnormal labels.
2) *Steam turbine dataset*[2]*:* The dataset consists of monitoring data obtained from SIS system of a million unit power plant, and these parameters are used for monitoring the health status of steam turbine. The boundary

[1]https://dataverse.harvard.edu/dataset.xhtml?persistentId=doi:10.7910/DVN/OPQMVF
[2]https://www.datafountain.cn/competitions/301

TABLE II
DESCRIPTIONS OF ALL EXPERIMENTAL DATASETS

Datasets	Number of training samples	Number of testing samples	Number of variables	Anomaly rate	Abnormal sequences	Abnormal dimensions
Satellite dataset	4100	857	32	75 (8.7%)	[300-360] [500-560] [700-760]	[1,15] [19,29] [22,25,29]
Steam turbine dataset	2828	1190	32	150 (12.6%)	[100-150] [500-550] [800-850]	[2,10,15,30] [12,19,28] [2,15,29]
Power consumption dataset	300	203	32	70 (34.4%)	[50-78] [130-200]	[2,24,25] [3,7,25]
Gamma detector dataset	20000	3857	32 (65)	420 (12.8%)	[1000-1080] [2000-2080] [2500-2580]	[10,12,25] [12,29,31] [2,5,19]
Wind turbine dataset	1500	1000	32	221 (22.1%)	[520-529]	[9,10]

of each parameter is described in this dataset, and the dataset contains 37 attributes.

3) *Power consumption dataset*[3]*:* This dataset is a time series dataset which represents the power consumption in different states of India. The time range of this dataset is from January 3, 2019 till May 23, 2020. This dataset is available on Kaggle.

Rows and columns put together, each data point reflects the power consumed in mega units (MU) by the given state (column) at the given date (row).

Gamma polarization detector dataset: This dataset is a real dataset collected from a gamma polarimetry detector of some Chinese Manned Space Flight Project. This detector broke down several minutes after the aircraft exits the South Atlantic Anomaly (SAA) region, and all 65 parameters of this dataset record this faulty event. Actually, we select 32 key dimensions of this dataset in our experiments.

Wind turbine dataset: This dataset is collected from the SCADA system of wind farm and the dataset has 32-dimension parameters. Most parameters are temperatures of different parts of the unit, and the remaining ones are wind speed, generator speed, active power, and other basic parameters of wind turbine. Typical mechanical faults can always cause the increase of specific temperature parameters. Hence, the dataset is marked with normal and abnormal labels.

B. Experimental Setup

We use open-source anomaly detection library pylof and DL framework PyTorch to develop the baseline models and CCG-EDGAN. The computer configuration is Intel(R) Xeon(R) CPU E5-2620 v4 2.10GHz with a 12G NVIDIA TITAN X (Pascal) GPU, 32G Memory.

Nine comparative algorithms are conducted to verify the superiority of CCG-EDGAN, including classical anomaly detection algorithms KNN [9], local outlier factor (LOF) [11], cluster-based local outlier factor (CBLOF), histogram-based outlier score (HBOS) [31], isolation forest (iForest) [32] and deep architecture, f-AnoGAN [22], GANomaly [24], MSCRED [7], and EGBAD [19]. The detailed information of comparative algorithms and CCG-EDGAN are illustrated in the Table III.

[3]https://www.kaggle.com/twinkle0705/state-wise-power-consumption-in-india?select=dataset_tk.csv

TABLE III
DETAILED INFORMATION OF ALL EXPERIMENTAL MODELS

Model	LR[1]	LR_{d}^{2}	LR_{g}^{3}	$Niter$[4]	BS[5]
KNN	×	×	×	×	×
LOF	×	×	×	×	×
CBLOF	×	×	×	×	×
HBOS	×	×	×	×	×
Isolation Forest	×	×	×	×	×
EGBAD	×	10^{-4}	10^{-4}	500	128
f-AnoGAN	×	10^{-5}	10^{-3}	500	128
GANomaly	×	10^{-5}	10^{-3}	500	128
MSCRED	10^{-4}	×	×	500	5
CCG-EDGAN	×	10^{-5}	10^{-3}	500	128

LR: Learning rate LR_D: Learning rate of the discriminator LR_G: Learning rate of the generator *Niter*: Number of training iterations *BS*: Batch size

C. Mode Evaluation

Considering the imbalance of normal and anomalous samples in anomaly detection task, three indexes including F_1 Score, Matthews correlation coefficient (MCC), and Fowlkes–Mallows (FM) [30] are adopted to evaluate the algorithm performance of anomaly detection. Meanwhile, the index correct rate (CR) and error rate (ER) are utilized to evaluate the performance of anomaly location.

1) F_1 *Score:* The harmonic average of precision and recall is between [0, 1]. The higher the value is, the better the algorithm performance is

$$F_1 = 2 \times \frac{\text{precision} \times \text{recall}}{\text{precision} + \text{recall}} \tag{9}$$

2) *MCC:* MCC is utilized to represent the correlation coefficient between actual classification and predicted

TABLE IV
EXPERIMENTAL RESULTS OF ANOMALY DETECTION ON FIVE DATASETS FOR ALL ALGORITHMS

Dataset	Satellite dataset			Steam turbine dataset			Power consumption dataset			Gamma detector dataset			Wind turbine dataset		
Algorithm	F1	MCC	FM	F_1	MCC	FM	F_1	MCC	FM	F_1	MCC	FM	F_1	MCC	FM
KNN	0.51	0.39	0.52	0.23	0.09	0.23	0.16	-0.06	0.20	0.64	0.63	0.67	0.78	0.73	0.78
LOF	0.14	0.1	0.14	0.15	-0.01	0.15	0.37	0.16	0.41	0.09	-0.03	0.1	0.02	-0.2	0.02
CBLOF	0.70	0.62	0.71	0.59	0.53	0.60	0.24	-0.08	0.26	0.59	0.60	0.64	0.67	0.58	0.67
HBOS	0.41	0.24	0.41	0.25	0.11	0.25	0.30	0.02	0.33	0.14	0.03	0.15	0.31	0.12	0.31
iForest	0.33	0.15	0.33	0.39	0.29	0.40	0.34	0.09	0.38	0.30	0.23	0.33	0.40	0.24	0.40
EGBAD	0.51	0.31	0.56	0.38	0.29	0.43	0.77	0.49	0.77	0.32	0.31	0.41	0.51	0.33	0.55
f-AnoGAN	0.74	0.65	0.75	0.72	0.68	0.73	0.92	0.85	0.92	0.57	0.56	0.61	0.66	0.56	0.69
GANomaly	**0.95**	**0.93**	**0.95**	0.54	0.58	0.61	0.94	0.89	0.94	0.80	0.80	0.82	0.78	0.72	0.80
MSCRED	0.94	0.92	0.94	0.69	0.65	0.69	0.95	0.90	0.95	0.70	0.68	0.70	0.72	0.65	0.72
CCG-EDGAN	0.93	0.91	0.93	**0.81**	**0.79**	**0.81**	**0.97**	**0.94**	**0.97**	**0.87**	**0.86**	**0.87**	**0.82**	**0.77**	**0.83**

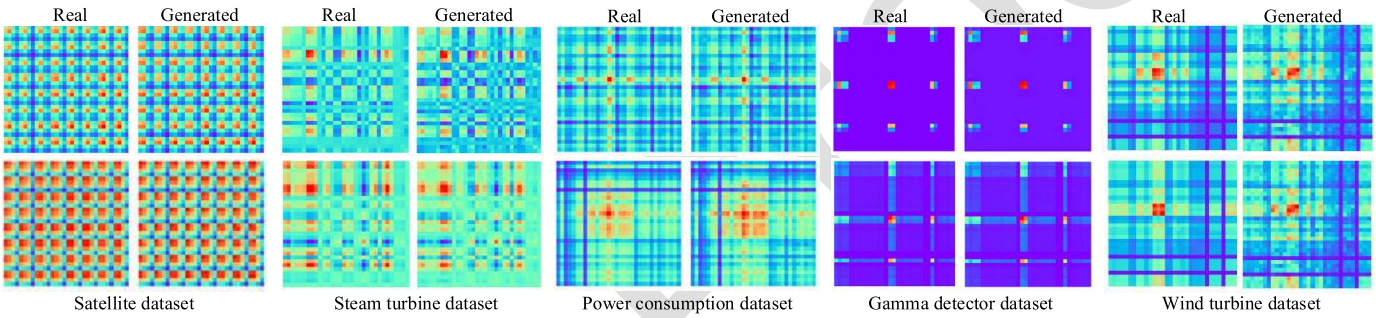

Fig. 2. Real and generated cross correlation graphs via CCG-EDGAN on five datasets.

classification. The range of MCC is $[-1, 1]$, and higher value means better classification result.

$$\mathrm{MCC} = \frac{\mathrm{TP}\times\mathrm{TN} - \mathrm{FP}\times\mathrm{FN}}{\sqrt{(\mathrm{TP}+\mathrm{FP})\times(\mathrm{TP}+\mathrm{FN})\times(\mathrm{TN}+\mathrm{FP})\times(\mathrm{TN}+\mathrm{FN})}}. \tag{10}$$

3) *FM:* FM is defined as the geometric mean of precision and recall. The higher the value is, and the better the algorithm performance is

$$\mathrm{FM} = \frac{\mathrm{TP}}{\sqrt{(\mathrm{TP}+\mathrm{FP})\times(\mathrm{TP}+\mathrm{FN})}}. \tag{11}$$

4) *CR and ER:* CR and ER are novelty designed to evaluate the anomaly location model, and higher CR value and smaller ER value represent better performance of anomaly location algorithm. It is noticed note that sum of CR and ER is not equal to 1

$$\mathrm{CR} = \frac{\text{number of correct location}}{\text{number of anomalies}} \tag{12}$$

$$\mathrm{ER} = \frac{\text{number of false location}}{\text{number of anomalies}} \tag{13}$$

D. Experimental Results

1) Anomaly Detection Results: In this section, we summarize the results of extensive experiments to analyze the anomaly detection performance of baseline algorithms and CCG-EDGAN. The experimental results on five datasets including the comparative analysis of F_1, MCC, and FM about baseline algorithms and CCG-EDGAN are given in Table IV. Generally speaking, traditional machine learning models perform worse than deep architectures when facing anomaly detection issue of multivariate time series. The results can also indicate that CCG-EDGAN can achieve better performance on Steam turbine, power consumption, gamma detector datasets, and wind turbine dataset, which demonstrate the proposed framework is an excellent model on most datasets for multivariate time series anomaly detection tasks.

For further investigation, we adopt visualization manner to show the effectiveness of CCG-EDGAN, especially on data reconstruction ability of the Generator, and the cross correlation graphs of real and generated data are shown in Fig. 2. The visualization heatmaps show high similarity between cross correlation graphs of real and generated data, which indicate that CCG-EDGAN has effectively learned the inner correlation characteristics of multivariate time series. Actually, the main reasons why CCG-EDGAN can achieve good performance in anomaly detection can be summarized as follows: 1) a multiple cost function is designed to restrain the optimization direction of CCG-EDGAN from the latent space and the original space simultaneously, contributing to improve the representation ability of the proposed framework; 2) the Generator of CCG-EDGAN can generate high-quality cross correlation graphs, which makes anomalous sequences can to be easily detected via reconstruction errors between normal and anomalous data.

2) Anomaly Location Results: In this article, because traditional machine learning algorithms and EGBAD do not have the ability of anomaly location, we only compare

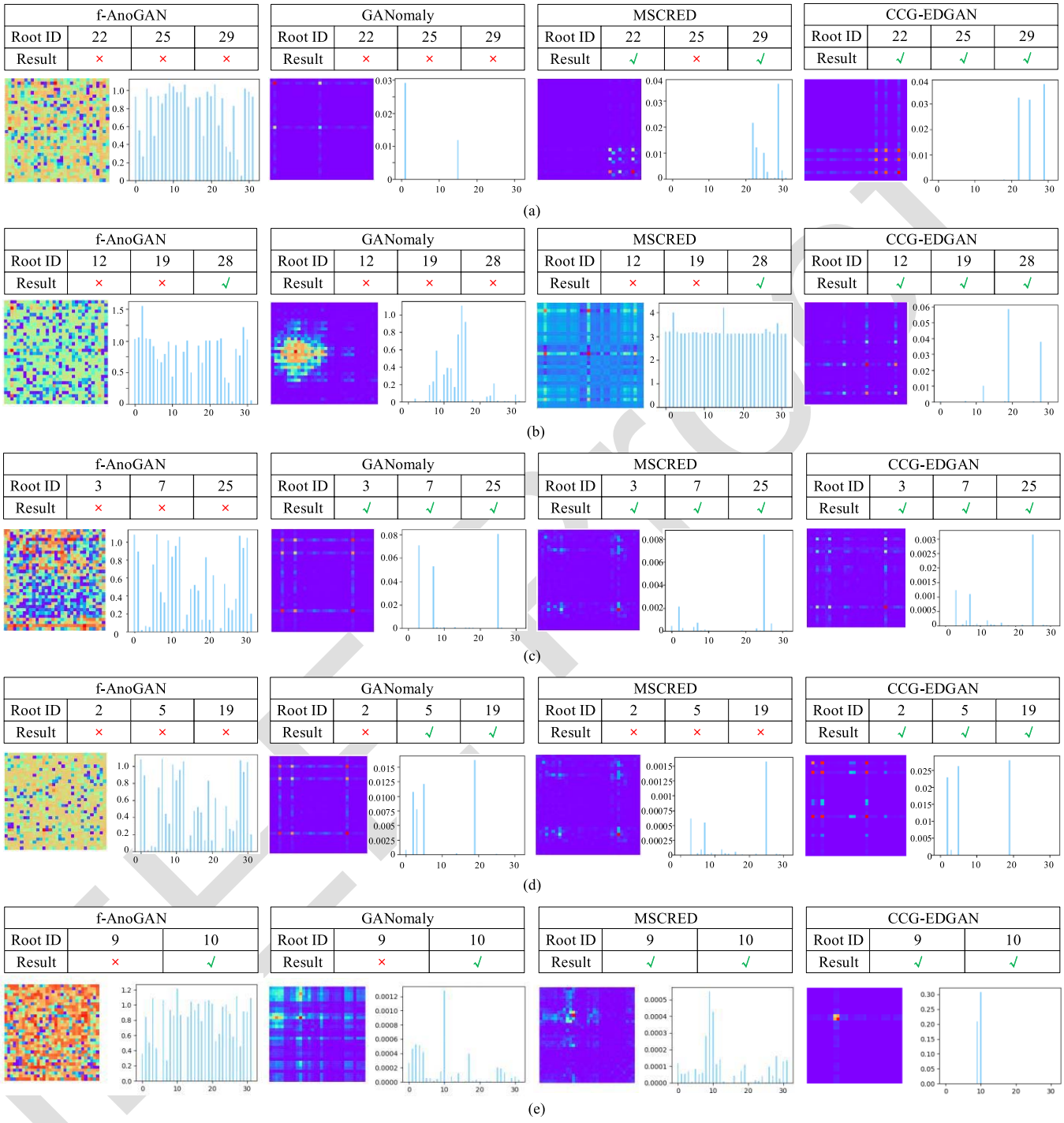

Fig. 3. Partial anomaly location results on five experimental datasets.

CCG-EDGAN with deep architecture algorithms (f-AnoGAN, GANomaly, and MSCRED) on anomaly location task. The comparative results including CR and error rate of baseline algorithms and CCG-EDGAN are shown in Table V. And therein correct indicates the number of anomalies which are successfully located. Error represents the number of anomalies that failed to locate (including false and missing data), and the equations of CR and ER are defined in (12) and (13). As shown in Table V, CCG-EDGAN achieves the best anomaly location performance on five datasets, providing reliable anomaly location results.

Partial anomaly location results of five datasets are shown in Fig. 3, the left subgraphs indicate the reconstruction errors matrix of testing samples, and the right ones show the statistical histogram of anomaly location results. Among the statistical histograms, the horizontal axis represents the serial number of multivariate time series dimensions, and the vertical axis represents error value for each dimension.

TABLE V
EXPERIMENTAL RESULTS OF ANOMALY LOCATION ON FIVE DATASETS FOR ALL ALGORITHMS

	Satellite dataset		Steam turbine dataset		Power consumption dataset		Gamma detector dataset		Wind turbine dataset	
	CR	ER	CR	ER	CR	ER	CR	ER	CR	ER
f-AnoGAN	0	0.88	0	0.88	0	0.91	0	0.85	0	0.95
GANomaly	0.49	0.47	0	0.37	0.94	0	0	0.15	0.92	0
MSCRED	0.31	0.64	0	0.6	0.41	0.53	0.03	0.73	0.55	0.10
CCG-EDGAN	**0.98**	**0**	**0.78**	**0.02**	**0.99**	**0**	**0.96**	**0**	**0.95**	**0**

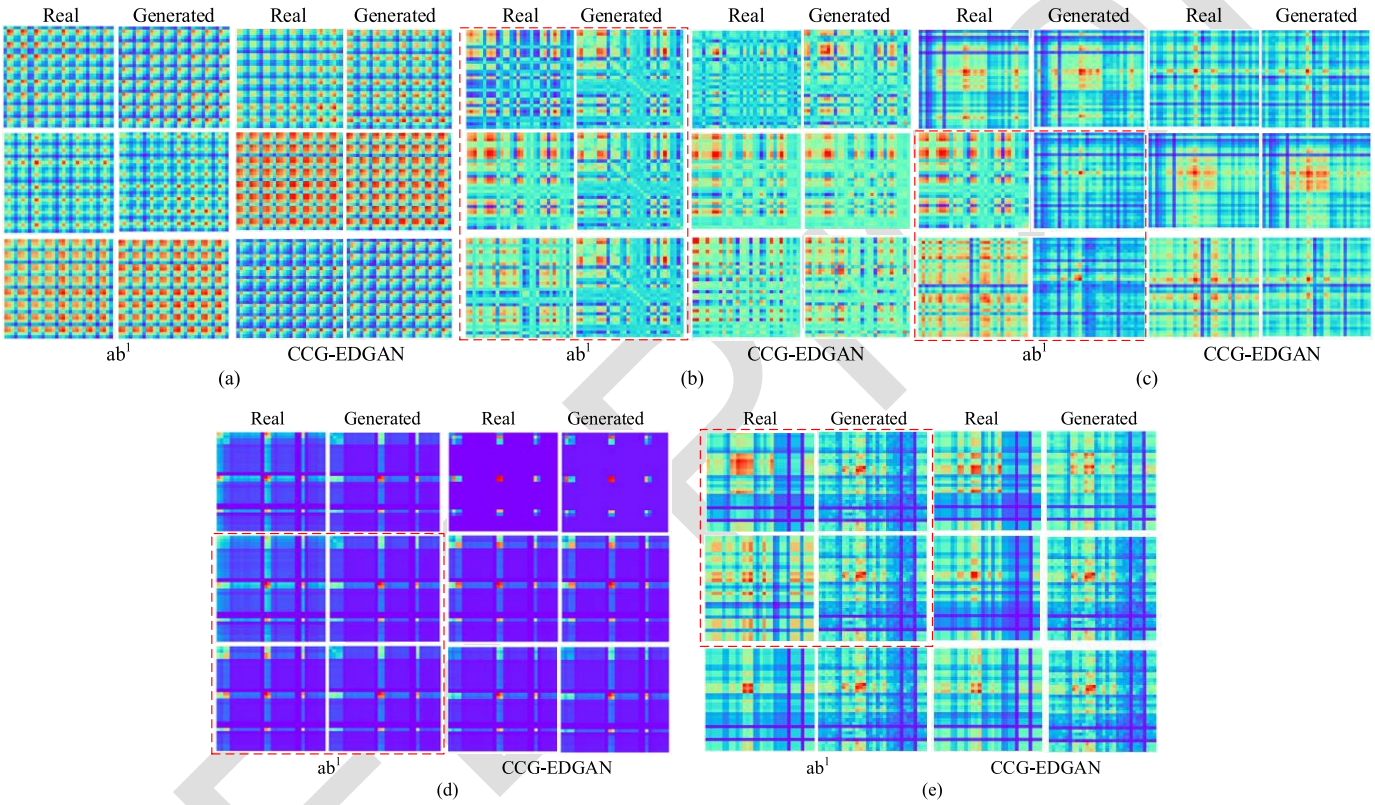

Fig. 4. Real and generated cross correlation graphs via CCG-EDGAN and model ab[1] in the first ablation study.

Therefore, greater value means greater occurrence probability of anomalies in corresponding dimension. We can see from anomaly location histograms, and CCG-EDGAN has excellent ability to distinguish anomalous dimensions of multivariate time series. Contrarily, histograms of baseline algorithms illustrate comparative models have poor anomaly detection performance, even if such models have good anomaly detection performance. As states, experimental results demonstrate that the proposed framework can achieve an excellent and consistent performance on anomaly detection and location tasks.

3) Ablation Study: In order to verify the effectiveness of noise module and residual connection, ablation studies are designed in this section. The proposed framework without noise module or residual connection is conducted. The noise module is used to increase the randomness of input for CCG-EDGAN, avoiding mode collapse during the data reconstruction. In the first ablation experiment, the noise module is removed from CCG-EDGAN (model ab[1]), and learned perceptual image patch similarity (LPIPS) [33] is utilized to evaluate the diversity of reconstruction data. LPIPS measured the average characteristic distance between reconstruction samples, and larger LPIPS value means better diversity of reconstruction samples. Therefore, the evaluation indicators of the first ablation study are F_1, MCC, FM, and LPIPS, shown in Table VI. The results indicate that noise module can effectively eliminate mode collapse of CGG-EDGAN framework, further improving its anomaly detection performance. Furthermore, the comparative heatmaps of model ab[1] and CGG-EDGAN are drawn to visually indicate the mode collapse phenomenon of model ab[1] in Fig. 4. We can see that mode collapse occurs on steam turbine, power consumption, gamma detector, and wind turbine datasets (marked in the red dotted box), especially on steam turbine dataset. It can come to a conclusion that noise module plays a promoting role in suppressing mode collapse and improving model training.

Furthermore, residual connection modules are adopted to improve the representation ability of deep architecture, which can help CCG-EDGAN to learn more effective characteristics. Therefore, in the second ablation study, residual

TABLE VI
RESULT OF THE FIRST ABLATION EXPERIMENT (CCG-EDGAN AND MODEL ab^1)

	Satellite dataset		Steam turbine dataset		Power consumption dataset		Gamma detector dataset		Wind turbine dataset	
	ab^1	CCG-EDGAN	ab^1	CCG-EDGAN	ab^1	CCG-EDGAN	ab^1	CCG-EDGAN	ab^1	CCG-EDGAN
F1	0.88	**0.93**	0.72	**0.81**	0.71	**0.97**	0.71	**0.87**	0.65	**0.82**
MCC	0.84	**0.91**	0.69	**0.79**	0.51	**0.94**	0.70	**0.86**	0.56	**0.77**
FM	0.88	**0.93**	0.72	**0.81**	0.72	**0.97**	0.72	**0.87**	0.65	**0.83**
LPIPS	0.0290	**0.0293**	1.75e-14	**0.049**	0.058	**0.0598**	1.47e-14	**0.0527**	0.02	**0.027**

TABLE VII
RESULT OF THE SECOND ABLATION EXPERIMENT (CCG-EDGAN AND MODEL ab^2)

	Satellite dataset		Steam turbine dataset		Power consumption dataset		Gamma detector dataset		Wind turbine dataset	
	ab^2	CCG-EDGAN	ab^2	CCG-EDGAN	ab^2	CCG-EDGAN	ab^2	CCG-EDGAN	ab^2	CCG-EDGAN
F1	0.37	**0.93**	0.73	**0.81**	**0.97**	**0.97**	0.76	**0.87**	0.68	**0.82**
MCC	0.37	**0.91**	0.70	**0.79**	**0.94**	**0.94**	0.74	**0.86**	0.56	**0.77**
FM	0.44	**0.93**	0.74	**0.81**	**0.97**	**0.97**	0.76	**0.87**	0.69	**0.83**
CR	0.24	**0.98**	0.65	**0.78**	0.97	**0.99**	0.80	**0.96**	0.83	**0.95**
ER	**0**	**0**	**0.013**	0.02	0.014	**0**	**0**	**0**	0.01	**0**

connection modules are removed from the proposed framework (model ab^2), and its effectiveness is evaluated in both anomaly detection and location via F_1, MCC, FM, CR, and ER indexes, as shown in Table VII. It is worth noting that the ER of model ab^2 on steam turbine dataset is lower. That is because the number of anomalies identified by model ab^2 is much less than CCG-EDGAN. In this case, the number of identified anomalies in anomaly location task through model ab^2 is also less, but it does not mean the performance of model ab^2 is better than that of the standard CCG-EDGAN, and less ER might result in higher false positive rate. This viewpoint can be verified by the other evaluation indicators on steam turbine dataset. Except for steam turbine dataset, standard CGG-EDGAN performs better than ab^2 on satellite, power consumption, gamma detector, and wind turbine datasets. In conclusion, the second ablation study shows that residual connection modules can effectively help CCG-EDGAN framework to learn more useful features and improve the performance of anomaly detection and location tasks.

V. CONCLUSION

In this article, a novel anomaly detection and location of multivariate time series method named CCG-EDGAN is proposed. Multivariate time series are transformed into cross correlation graphs through multitime scale sliding window-based correlation computation. And then cross correlation graphs are fed into encoder–decoder GAN structure to learn the correlation features of cross correlation graphs. Besides, multiple loss items discriminator loss, feature matching loss, encoding loss, and reconstruction loss are designed to create a cost function to enhance the representation ability of CCG-EDGAN, contributing to better detect and locate the unusual change of inner features in multivariate time series. Furthermore, reconstruction matrix deviation in original space from encoder–decoder structure is used to provide a consistent indicator for anomaly detection and location, avoiding the inconsistent performances on detection and location tasks.

Extensive experiments on three datasets and two real industrial datasets are conducted to verify the effectiveness of the proposed framework. Results indicate that our framework can provide a generic, excellent, and consistent framework for anomaly detection and location of multivariate time series. Extra ablation studies can verify that noise module can slow down mode collapse of GAN architecture, and residual connection module is conducive to help deep architecture to achieve better convergence performance. Our future work aims to improve the computation efficiency of CGG-EDGAN or investigate parallel deployment of deep model, supporting the application demands of streaming data monitoring in industrial fields.

REFERENCES

[1] S. Du, T. Li, Y. Yang, and S.-J. Horng, "Multivariate time series forecasting via attention-based encoder–decoder framework," *Neurocomputing*, vol. 388, pp. 269–279, May 2020.

[2] J. Yu, Y. Song, D. Tang, D. Han, and J. Dai, "Telemetry data-based spacecraft anomaly detection with spatial–temporal generative adversarial networks," *IEEE Trans. Instrum. Meas.*, vol. 70, pp. 1–9, 2021.

[3] L. Yang, Z. Han, J. Zhong, C. Li, and Z. Liu, "A generic anomaly detection of catenary support components based on generative adversarial networks," *IEEE Trans. Instrum. Meas.*, vol. 69, no. 5, pp. 2439–2448, Nov. 2019.

[4] M. Fu, J. Liu, D. Zang, and S. Lu, "Anomaly detection of complex MFI measurements using low-rank recovery in pipeline transportation inspection," *IEEE Trans. Instrum. Meas.*, vol. 69, no. 9, pp. 6776–6786, Feb. 2020.

[5] A. L. Ellefsen, P. Han, X. Cheng, F. T. Holmeset, V. Aesoy, and H. Zhang, "Online fault detection in autonomous ferries: Using fault-type independent spectral anomaly detection," *IEEE Trans. Instrum. Meas.*, vol. 69, no. 10, pp. 8216–8225, Oct. 2020.

[6] N. Chawla, N. Japkowicz, and A. Kotcz, "Special issue on learning from imbalanced data sets," in *Proc. ACM SIGKDD Explor. Newslett.*, 2004, pp. 1–6.

[7] C. Zhang *et al.*, "A deep neural network for unsupervised anomaly detection and diagnosis in multivariate time series data," in *Proc. AAAI Conf. Artif. Intell.*, Jul. 2019, pp. 1409–1416.

[8] M. Goldstein and S. Uchida, "A comparative evaluation of unsupervised anomaly detection algorithms for multivariate data," *PLoS ONE*, vol. 11, no. 4, Apr. 2016, Art. no. e0152173.

[9] V. Hautamaki, I. Karkkainen, and P. Franti, "Outlier detection using k-nearest neighbour graph," in *Proc. 17th Int. Conf. Pattern Recognit. (ICPR)*, Aug. 2004, pp. 430–433.

[10] E. Bigdeli, B. Raahemi, M. Mohammadi, and S. Matwin, "A fast noise resilient anomaly detection using GMM-based collective labelling," in *Proc. Sci. Inf. Conf. (SAI)*, Jul. 2015, pp. 337–344.

[11] X. Miao, Y. Liu, H. Zhao, and C. Li, "Distributed online one-class support vector machine for anomaly detection over networks," *IEEE Trans. Cybern.*, vol. 49, no. 4, pp. 1475–1488, Apr. 2018.

[12] D. Liu *et al.*, "Opprentice: Towards practical and automatic anomaly detection through machine learning," in *Proc. Internet Meas. Conf.*, Oct. 2015, pp. 211–224.

AQ:3

[13] N. Laptev, S. Amizadeh, and I. Flint, "Generic and scalable framework for automated time-series anomaly detection," in *Proc. 21th ACM SIGKDD Int. Conf. Knowl. Discovery Data Mining*, Aug. 2015, pp. 1939–1947.
[14] H. Xu *et al.*, "Unsupervised anomaly detection via variational auto-encoder for seasonal KPIs in web applications," in *Proc. World Wide Web Conf. World Wide Web (WWW)*, 2018, pp. 187–196.
[15] Z. Li, Y. Zhao, R. Liu, and D. Pei, "Robust and rapid clustering of KPIs for large-scale anomaly detection," in *Proc. IEEE/ACM 26th Int. Symp. Quality Service (IWQoS)*, Jun. 2018, pp. 1–10.
[16] G. Pang, C. Shen, L. Cao, and A. Hengel, "Deep learning for anomaly detection: A review," *ACM Comput. Surv.*, vol. 54, no. 2, pp. 1–38, 2021.
[17] Z. Niu, K. Yu, and X. Wu, "LSTM-based VAE-GAN for time-series anomaly detection," *Sensors*, vol. 20, no. 13, p. 3738, Jul. 2020.
[18] W. Jiang, Y. Hong, B. Zhou, X. He, and C. Cheng, "A GAN-based anomaly detection approach for imbalanced industrial time series," *IEEE Access*, vol. 7, pp. 143608–143619, 2019.
[19] H. Zenati, C. Sheng Foo, B. Lecouat, G. Manek, and V. R. Chandrasekhar, "Efficient GAN-based anomaly detection," 2018, *arXiv:1802.06222*.
[20] D. Li, D. Chen, B. Jin, L. Shi, J. Goh, and S.-K. Ng, "MAD-GAN: Multivariate anomaly detection for time series data with generative adversarial networks," in *Proc. Int. Conf. Artif. Neural Netw.*, 2019, pp. 703–716.
[21] C. Zhang *et al.*, "A deep neural network for unsupervised anomaly detection and diagnosis in multivariate time series data," in *Proc. AAAI Conf. Artif. Intell.*, vol. 33, no. 1, pp. 1409–1416, Jul. 2019.
[22] T. Schlegl *et al.*, "Unsupervised anomaly detection with generative adversarial networks to guide marker discovery," in *Proc. Int. Conf. Inf. Process. Med. Imag.* Cham, Switzerland: Springer, 2017, pp. 146–157.
[23] T. Schlegl, P. Seeböck, S. M. Waldstein, G. Langs, and U. Schmidt-Erfurth, "F-AnoGAN: Fast unsupervised anomaly detection with generative adversarial networks," *Med. Image Anal.*, vol. 54, pp. 30–44, May 2019.
[24] S. Akcay, A. Atapour-Abarghouei, and T. P. Breckon, "GANomaly: Semi-supervised anomaly detection via adversarial training," in *Proc. Asian Conf. Comput. Vis.* Cham, Switzerland: Springer, 2018, pp. 622–637.
[25] D. Hallac, S. Vare, S. Boyd, and J. Leskovec, "Toeplitz inverse covariance-based clustering of multivariate time series data," in *Proc. 27th Int. Joint Conf. Artif. Intell.*, Jul. 2018, pp. 215–223.
[26] G. Jiang, H. Chen, and K. Yoshihira, "Efficient and scalable algorithms for inferring likely invariants in distributed systems," *IEEE Trans. Knowl. Data Eng.*, vol. 19, no. 11, pp. 1508–1523, Nov. 2007.
[27] H. Liang, L. Song, J. Wang, L. Guo, X. Li, and J. Liang, "Robust unsupervised anomaly detection via multi-time scale DCGANs with forgetting mechanism for industrial multivariate time series," *Neurocomputing*, vol. 423, pp. 444–462, Jan. 2021.
[28] C. Yin, S. Zhang, J. Wang, and N. N. Xiong, "Anomaly detection based on convolutional recurrent autoencoder for IoT time series," *IEEE Trans. Syst., Man, Cybern. Syst.*, vol. 52, no. 1, pp. 112–122, Jan. 2022.
[29] K. Deepak, S. Chandrakala, and C. K. Mohan, "Residual spatiotemporal autoencoder for unsupervised video anomaly detection," *Signal, Image Video Process.*, vol. 15, no. 1, pp. 215–222, Feb. 2021.
[30] K. H. Brodersen, C. S. Ong, K. E. Stephan, and J. M. Buhmann, "The balanced accuracy and its posterior distribution," in *Proc. 20th Int. Conf. Pattern Recognit.*, Aug. 2010, pp. 3121–3124.
[31] V. Chandola, A. Banerjee, and V. Kumar, "Anomaly detection: A survey," *ACM Comput. Surv.*, vol. 41, no. 3, pp. 1–58, Jul. 2009.
[32] F. T. Liu, K. M. Ting, and Z.-H. Zhou, "Isolation forest," in *Proc. 8th IEEE Int. Conf. Data Mining*, Dec. 2008, pp. 413–422.
[33] R. Zhang, P. Isola, A. A. Efros, E. Shechtman, and O. Wang, "The unreasonable effectiveness of deep features as a perceptual metric," in *Proc. IEEE/CVF Conf. Comput. Vis. Pattern Recognit.*, Jun. 2018, pp. 586–595.

Haoran Liang received the B.Eng. degree from the North China University of Technology, Beijing, China, in 2016. He is currently pursuing the Ph.D. degree with the University of Chinese Academy of Sciences, Beijing.

His current research interests include deep learning, anomaly detection, and time series representational learning.

Lei Song received the Ph.D. degree in thermal energy engineering from North China Electric Power University, Beijing, China, in 2015.

He is currently an Associate Researcher with the Data Analysis Group, Payload Operation and Control Center, Technology and Engineering Center for Space Utilization, Chinese Academy of Sciences, Beijing. His current research interests include failure analysis, anomaly detection, condition monitoring, life prediction, and their application to mechanical system in aerospace and energy engineering.

Junrong Du received the Digital Media Technology degree from Yanbian University, Yanji, China, in 2018. She is currently pursuing the Ph.D. degree with the University of Chinese Academy of Sciences, Beijing, China.

Her current research interests include machine learning, transfer learning, and remaining useful life prediction.

Xuzhi Li received the B.S. degree from Peking University, Beijing, China, in 1990, and the M.S. degree from the National Space Science Center, Beijing, in 1993.

His current research interests include ground system engineering, integrated information technology, and intelligent information processing.

Lili Guo received the B.S. and M.S. degrees in computer science and technology from Xi'an Jiao tong University, Xi'an, China, in 1996 and 2002, respectively.

From 2002 to 2010, she worked with the Academy of Opto-Electronics, Chinese Academy of Sciences. She is currently a Professor with the Key Laboratory of Space Utilization, Technology and Engineering Center for Space Utilization, Chinese Academy of Sciences. Her main research interests include data mining and software engineering.